American Journal of Engineering Research (AJER)
e-ISSN: 2320-0847 p-ISSN : 2320-0936
Volume-5, Issue-4, pp-38-45
www.ajer.org
Research Paper Open Access

Numerical Simulation and Experimental Investigation of Rectangular Waveguide Electrical Field Taking Into Account Nonlinear Means

E.G.Ismibayli, I.J.Islamov, R.Sh.Abdullayev
Department of Radio Engineering and Telecommunication Azerbaijan Technical University Baku, Azerbaijan

ABSTRACT: *Some new mathematical models of the electric field of a rectangular waveguide (RW) filled with air have been developed, taking the nonlinearity of the medium into account, which are described by partially differential equations of elliptic type. By using the finite difference method it has been determined the actual value of the electric field tension of RW with air filling. An experimental study has been conducted, as a result of which, the values of the electric field of the studied device have been set. The comparison of the results of calculations and experiment have been conducted, which is quite satisfactory, and the error does not exceed 5%.*
Keywords: *microwave, rectangular waveguide, electrical field, numerical method.*

I. INTRODUCTION

Intensive development of the art of ultrahigh frequency (UHF) entailed the creation of simple compact transmission lines, as the latter is largely determined by the electric and structural parameters of radio devices in which they are applied.

Recently RW with air filling have been widespread in practice from varieties of microwave transmission lines. These transmission lines are over broadband, cheaper and easier to manufacture, have a high dielectric strength required for the transmission of high power, high mechanical strength, providing high reliability, long life and resistance to mechanical stress, minimal power loss, thereby increasing the range of radio activities and improved electrical characteristics and elements of radio nodes, constructed on the basis of RW with air filling.

A considerable number of theoretical works have been devoted for the calculation of the electric field inside of RW. It should be noted that even with the necessary credibility and value, the obtained theoretical data is only valid for the linear medium. However, when the strong electric field inside of RW fields filled with air it is circulated in the nonlinear space [1-5]. Therefore, the problem of numerical calculation and experimental study inside of the electric field with RW filled with air, with all the factors listed above, is not solved so far and is significant in electrodynamics.

II. DEVELOPMENT OF MATHEMATICAL MODELS OF THE ELECTRIC FIELD

It is known that for the electric field, the vector divergence of the electric induction $\vec{D}$ at the point within the volume is equal to the density of charge ρ, that is, [6-9]:

$$div\,\vec{D} = \rho. \qquad (1)$$

From the other hand [10]

$$\vec{D} = \varepsilon\varepsilon_0 \vec{E}, \qquad (2)$$

$$\vec{E} = -grad\ \varphi, \qquad (3)$$

here φ – is scalar electric potential, ε – relative permittivity, $\vec{E}$ – vector of the electric field strength, $\varepsilon_0 = 8,85 \cdot 10^{-12}\, F/m$ electric constant.
Substituting (3) in the expression (1) taking into account the equation (2), we obtain:

$$\nabla^2 \varphi = -\frac{\rho}{\varepsilon\varepsilon_0}, \quad (4)$$

here ∇ – is a differential operator of nose $\nabla^2 = \frac{\partial^2}{\partial x^2} + \frac{\partial^2}{\partial y^2} + \frac{\partial^2}{\partial z^2}$.
Transforming the left-hand side of equation (4), we find:

$$\frac{\partial}{\partial x}\left(\varepsilon \frac{\partial \varphi}{\partial x}\right) + \frac{\partial}{\partial y}\left(\varepsilon \frac{\partial \varphi}{\partial y}\right) + \frac{\partial}{\partial z}\left(\varepsilon \frac{\partial \varphi}{\partial z}\right) = -\frac{\rho}{\varepsilon_0}. \quad (5)$$

When $\varepsilon = \varepsilon(E)$, the equation (5) takes the following form:

$$\frac{\partial}{\partial x}\left[\varepsilon(E) \frac{\partial \varphi}{\partial x}\right] + \frac{\partial}{\partial y}\left[\varepsilon(E) \frac{\partial \varphi}{\partial y}\right] + \frac{\partial}{\partial z}\left[\varepsilon(E) \frac{\partial \varphi}{\partial z}\right] = -\frac{\rho}{\varepsilon_0}. \quad (6)$$

In strong fields, we find a relationship between the relative dielectric constant ε and the electric field E, for which we use the following graph [11-14]:

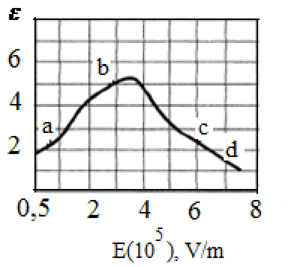

Fig.1 The relationship between the relative permittivity ε and the electric field strength E.

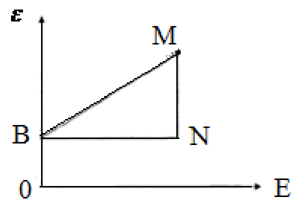

Fig.2 Definition of the analytical expression between ε and E.

It should be noted that, when a strong field strength, as in our case, the medium has a nonlinear character. In a nonlinear medium, the dependence between the relative dielectric constant ε and the electric field ε is not linear [15-17].
As seen from figure 1, the relationship between ε and E field in the region of ab can be considered linear and wherein ε is defined as follows:

$$\varepsilon = \varepsilon_1 + kE, \quad (7)$$

here k-is the angular coefficient.

We lay off segment OB on the axis $o\varepsilon$ the value of which is equal to 1,8 and construct a straight line given by the equation (7) (fig.2). We draw segment OE through the point B parallel to the axis, whose value $BN = 3 \cdot 10^5$, and through point N segment $o\varepsilon$ parallel to the axis N whose value $NM = 3,2$. Then we draw line BM, which is the required one. It has a slope of $k = 3,2/3 \cdot 10^5$ and cuts on $o\varepsilon$ axis, the segment size $\varepsilon = 1,8$. Thus, by substituting the above data in (7), we obtain:

$$\varepsilon = 1,8 + 1,066 \cdot 10^{-5} E. \quad (8)$$

Substituting equation (8) into (6) we obtain

$$\frac{\partial}{\partial x}\left[(1,8 + 1,066 \cdot 10^{-5} E) \frac{\partial \varphi}{\partial x}\right] + \frac{\partial}{\partial y}\left[(1,8 + 1,066 \cdot 10^{-5} E) \frac{\partial \varphi}{\partial y}\right] +$$

$$+ \frac{\partial}{\partial z}\left[(1,8 + 1,066 \cdot 10^{-5} E) \frac{\partial \varphi}{\partial z}\right] = -\frac{\rho}{\varepsilon_0}. \quad (9)$$

III. NUMERICAL METHOD OF CALCULATION

In the calculation of the electric field in a certain homogeneous bounded domain V from a given source distribution field, it is necessary that its solution should satisfy the boundary conditions on the surface of S, bounding area V. Equation (9) belongs to the elliptic type. The ellipticity of the equation (9) takes place under certain conditions [18-20]. Therefore, a simple boundary value problem for the calculation of the field in the region V is the satisfaction of the Dirichlet conditions

$$\varphi(x, y, z) = \varphi_0(x, y, z). \tag{10}$$

Substituting the boundary conditions (tasks) for the equation (9), it is necessary to add the capacity of the regularity condition at infinity to the expression (10)

$$\lim_{(x^2+y^2+z^2)\to\infty} \varphi(x, y, z) < \infty. \tag{11}$$

It should be noted that the numerical solution of differential equations with partial derivatives (9) is algebraization of the problem, i.e., in this choice of a certain approximation of the solution and the differential operator, where the unknown coefficients in the approximated solution are determined from the system of algebraic equations.

In recent years, the general theoretical basis for almost all the methods used to calculate the electric field parameters it has become the finite difference method [21], which is one of the most effective and widely used methods of solution of initial, boundary and initial value problems for differential equations in partial derivatives.

Finite difference method is used quite successfully and is currently used for a wide range of problems of calculation of physical fields and processes and, in particular, electrical.
In the case of a nonlinear medium in the development of numerical algorithm, it is advisable to start from the field equations in the integral form. Therefore, the equation (9) can usefully lead to an integral form. Construction of a difference scheme of a nonlinear boundary value problem with respect to the component φ of the scalar electric potential, which describes the distribution of electric field in the region Q is shown in fig.3.

In order to solve the equation (9) it is necessary to know the initial and boundary conditions for the vector $\vec{E}$, for the scalar electric potential φ:

$$\begin{aligned} &\frac{\partial \varphi}{\partial y} = \alpha_1(x) && in\ region\ 1-4, \\ &\frac{\partial \varphi}{\partial y} = 0 && in\ region\ 1-2, \\ &\varphi = \chi && in\ region\ 2-3, \\ &\varphi = \alpha_2(x) && in\ region\ 3-4, \end{aligned} \tag{12}$$

here, $\alpha_1(x), \alpha_2(x)$ - defined functions, $\chi = const$, also an unknown quantity.
At the internal borders of the environment, the condition of continuity is maintained.

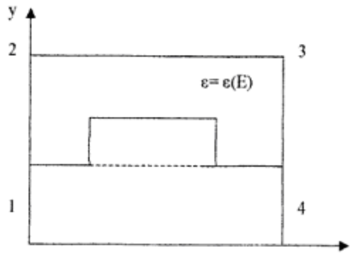

Fig.3 Estimated area: 1-4 nodes.

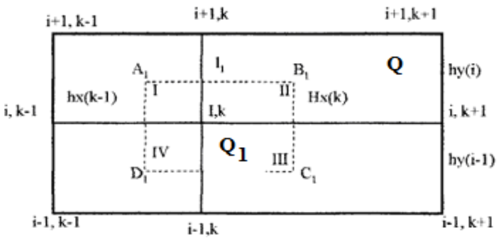

Fig.4 Inner node of grid: I-IV-subdomain.

In order to simplify the calculations, let us turn to the two-dimensional distribution of the electric field inside the RW with air filling. By using the law of total current and applying the relation

$$\begin{cases} E_x = -\varepsilon(E)\dfrac{\partial\varphi}{\partial y} = -\left(1,8+1,066\cdot 10^{-5}E\right)\dfrac{\partial\varphi}{\partial y}, \\ E_y = -\varepsilon(E)\dfrac{\partial\varphi}{\partial x} = -(1,8+1,066\cdot 10^{-5}E)\dfrac{\partial\varphi}{\partial x}, \end{cases} \qquad (13)$$

we obtain the equation (9) for the two-dimensional electric field in an integral form

$$\int_l (1,8+1,066\cdot 10^{-5}E)\frac{\partial\varphi}{\partial y}dx + \int_l (1,8+1,066\cdot 10^{-5}E)\frac{\partial\varphi}{\partial x}dy = \frac{1}{\varepsilon_0}\iint_Q \rho\, dxdy. \qquad (14)$$

In the computational domain Q (fig.4), we introduce an irregular grid with step $hx(k)$, $k = 1,2..,\ n_1 - 1,\ h$ y (i), i = 1,2,..., $n_2 - 1$ (n_1 - the number of nodes on the OX-axis, n_2 -number of nodes on the OY-axis), so that the lines forming the grid area, held by internal and external boundaries between media, and denote it by $\overline{Q}$. Lets consider an arbitrary inner grid node $\overline{Q}(i,k)$ (fig.4). Suppose the node (i,k) is in the range Q_1, limited with line $l_1(A_1B_1C_1D_1)$. Assuming [8], that within the grid cell space charge density and electric field strength are unchanged, we calculate the integrals on the left and right sides of the equation (14) in the area of Q_1, gamma, limited with line $l_1(A_1B_1C_1D_1)$.

$$\varphi_{i,k} = \frac{I + \gamma_1\varphi_{i-1,k} + \gamma_2\varphi_{i,k+1} + \gamma_3\varphi_{i,k-1} + \gamma_4\varphi_{i+1,k}}{\gamma_1 + \gamma_2 + \gamma_3 + \gamma_4}, \qquad (15)$$

$$\begin{cases} \gamma_1 = \dfrac{(1,8+1,066\cdot 10^{-5}E_{i,k-1})hx(k-1) + (1,8+1,066\cdot 10^{-5}E_{i,k})hx(k)}{2hy(i)}, \\ \gamma_2 = \dfrac{(1,8+1,066\cdot 10^{-5}E_{i-1,k})hy(i-1) + (1,8+1,066\cdot 10^{-5}E_{i,k})hy(i)}{2h(x)}, \\ \gamma_3 = \dfrac{(1,8+1,066\cdot 10^{-5}E_{i-1,k-1})hy(i-1) + (1,8+1,066\cdot 10^{-5}E_{i,k-1})hy(i)}{2hx(k-1)}, \\ \gamma_4 = \dfrac{(1,8+1,066\cdot 10^{-5}E_{i-1,k-1})hx(k-1) + (1,8+1,066\cdot 10^{-5}E_{i-1,k})hx(k)}{2hy(i-1)}, \end{cases} \qquad (16)$$

$$\begin{gathered} I = I_1 hx(k-1)hy(i)/4 + I_{II} hx(k)hy(i)/4 + \\ + I_{III} hx(k)hy(i-1)/4 + I_{IV} hx(k-1)hy(i-1)/4. \end{gathered} \qquad (17)$$

Accordingly, the strength of the electrical field in the point

$$\chi_2\left(y_i + \frac{hy(i)}{2},\ x_k + \frac{hx(k)}{2}\right)$$

is determined with the formulas:

$$E_x = \frac{\varphi_{i,k+1} - \varphi_{i+1,k+1} + \varphi_{i,k} - \varphi_{i+1,k}}{2hy(i)}, \qquad (18)$$

$$E_y = \frac{\varphi_{i+1,k+1} - \varphi_{i,k} + \varphi_{i,k+1} - \varphi_{i+1,k}}{2hx(k)}. \qquad (19)$$

According to the formula (15) it is possible to determine the value of the potential in any internal node of the grid area from the values of the potential in the four neighboring nodes.

Various boundary conditions (12) are set in the various nodes of the boundaries of the computational domain Q (fig.3). For all sections of the border and the corner points of the area, it is necessary to obtain their difference equations. On the part of the boundary 3-4 Dirichlet condition $\varphi = \alpha_2(x)$. In this case, the potential of the boundary node is determined once as the value of function $\alpha_2(y)$ at the point $y_{i,n1}$. In each node of the boundary area 2-3, the value of potential remains unchanged and equal to χ. Symmetry condition $\partial\varphi / \partial x = 0$ is set on the part of the boundary 1-2. In order to bypass the boundary node, in this case, we choose the path $l_4(A_4 B_4 C_4 D_4)$ (fig.5, v). Calculating the integrals on both sides of the expression (14), along the path $l_4(A_4 B_4 C_4 D_4)$ and the area Q_4, we get

$$\varphi_{i,1} = \frac{\gamma_1 \varphi_{i-1,1} + \gamma_2 \varphi_{i,2} + \gamma_4 \varphi_{i+1,1}}{\gamma_1 + \gamma_2 + \gamma_4}, \qquad (20)$$

here

$$\gamma_1 = \frac{(1,8 + 1,066 \cdot 10^{-5} E_{i-1,1})hx(1)}{2hy(i)}, \; \gamma_2 = \frac{(1,8 + 1,066 \cdot 10^{-5} E_{i-1,1})hy(i-1) + (1,8 + 1,066 \cdot 10^{-5} E_{i,1})hy(i)}{2hx(1)},$$

$$\gamma_3 = 0, \; \gamma_4 = \frac{(1,8 + 1,066 \cdot 10^{-5} E_{i-1,1})hx(1)}{2hy(i-1)}.$$

Let us consider the case where the condition is set in the area of boundaries in the form

$$\left.\frac{\partial x}{\partial y}\right|_{1-4} = \alpha_1(x).$$

The integration contour is selected in such a way that its lower part is held at the border of the computational domain $l_3(A_3 B_3 C_3 D_3)$ (fig.5, b).

If we lead integration along contour $l_3(A_3 B_3 C_3 D_3)$, we shall receive

$$\varphi_{1,k} = \frac{\gamma_2 \varphi_{2,k} + \gamma_1 \varphi_{1,k+1} + \gamma_4 \varphi_{3,k} - \gamma}{\gamma_2 + \gamma_3 + \gamma_4}, \qquad (21)$$

here $\gamma = \int_{x_k + \frac{hx(k-1)}{2}}^{x_k + \frac{hx(k)}{2}} \alpha_1(x)dx; \gamma_1 = 0; \gamma_2 = \frac{hy(1)}{2hx(k)}; \gamma_3 = \frac{hy(1)}{2hx(k-1)}; \gamma_4 = \frac{hx(k-1) + hx(k)}{2hy(1)}.$

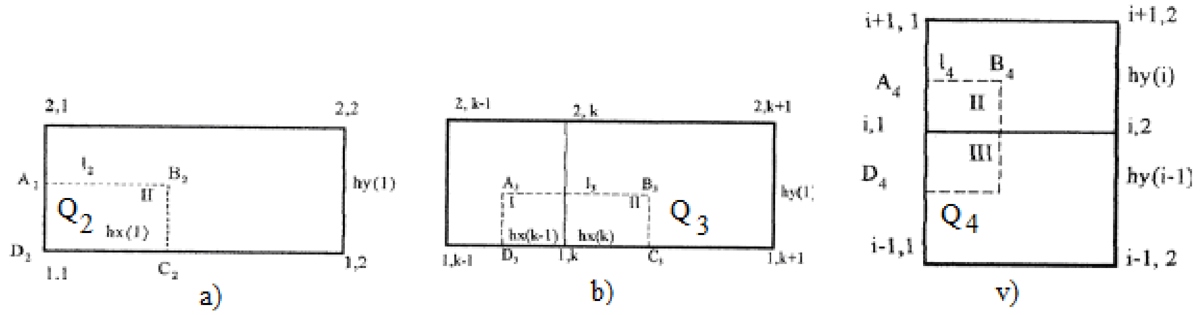

Fig.5 Boundary nodes of grid.

For a corner point 1 (fig.3)

$$\varphi_{1,1} = \frac{\gamma_2 \varphi_{1,2} + \gamma_4 \varphi_{2,1} - \gamma}{\gamma_2 + \gamma_4}. \qquad (22)$$

Here, the path of integration $l_3(A_2 B_2 C_2 D_2)$ (fig.5, a):

$$\gamma_1 = 0, \gamma_2 = \frac{hy\,(1)}{2\,hx\,(1)}, \gamma_3 = 0, \gamma_4 = \frac{hx\,(1)}{2\,hy\,(1)}, \gamma = \int_{x_1}^{x_1 + \frac{hx\,(1)}{2}} \alpha_1(x)dx.$$

The differential equation has the following form in point 4 (fig.3):

$$\varphi_{1,n_1} = \frac{\gamma_1 \varphi_{2,n_1} + \gamma_3 \varphi_{2,n_1} - \gamma}{\gamma_1 + \gamma_3}. \qquad (23)$$

Here, the integration contour l_5 is symmetrical to the contour shown in fig.5, a:

$$\gamma_1 = \frac{hx(n_1-1)}{2hy(1)}, \gamma_2 = 0, \gamma_3 = \frac{hy(1)}{2hx(n_1-1)}, \gamma_4 = 0, \gamma = \int_{x_{n1}\frac{hx(n_1-1)}{2}}^{xn_1} \alpha_1(x)dx.$$

Equations (15) and (20), (21) and (23) form a difference scheme of the boundary problem (9), (12), (14) of the system of algebraic equations, and they should be solved using iterative methods, in particular by successive upper relaxation (Young's method), because this method is extremely simple and easy to implement.

IV. CALCULATION OF THE FIELD STRENGTH

Based on the above mathematical algorithm design, calculation program is made in the language C^{++} and it was conducted a calculation method of the electric strength of the field RW with air-filling operating at frequencies 4,9-7,05 GHz, excitation with E-type and H-type waves. The dependences between the electric field intensity and the length of the cross section of RW with air filling for the E-type and H-type wave (fig.6 a, b) has been set. These relationships allow us to determine the electric field distribution inside the device. It should be noted that the data of the dependence also allows to determine the relationship between the electromagnetic and the design parameters of the studied device.

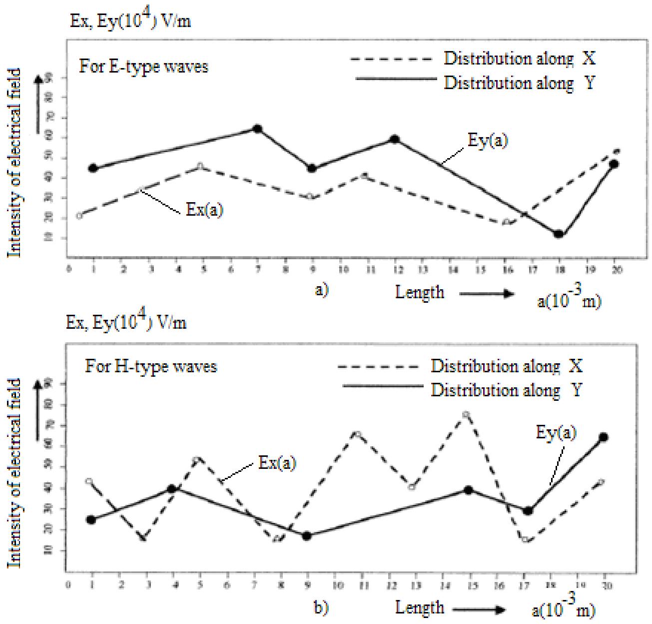

Fig. 6 Electric field dependence on the length of the cross-sectional RW with air filling for E-type (a) and the H-type (b) of the waves.

V. RESULTS OF EXPERIMENTAL STUDIES AND OF THEIR DISCUSSION

The experiment [3, 22] was conducted to determine the structure of the electric field inside of the RW with air filling, as well as to test the resulting differential equation with partial derivatives (9). Block diagram of the experimental setup is shown in fig.7.

On RW filling with air n = 20 hole was penetrated, which pickup probe is penetrated inside, wherein the distribution is measured along the wave guide.

Initiation of RW is generated with microwave generator operating in a range of 1 ÷ 10 cm. The currents in the excitatory vibrators may coincide in the direction or be opposite depending on the choice of the lengths of the power supply. These lengths can be made equal or differ with the half of the wave length in the cable.

The electric field is measured using a capacitance probe, which is a coaxial line open in one end, an inner conductor which acts on a specific length.

Frequency of UHF generator is set on the scale of the generator is controlled by wave meter accurately.

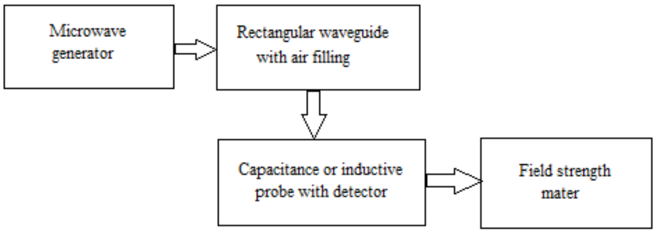

Fig.7 Block diagram of the experimental setup for measuring the field strength.

In experimental studies of the electric field inside of RW with air filling it was set tension of the electric field on portions of the device.

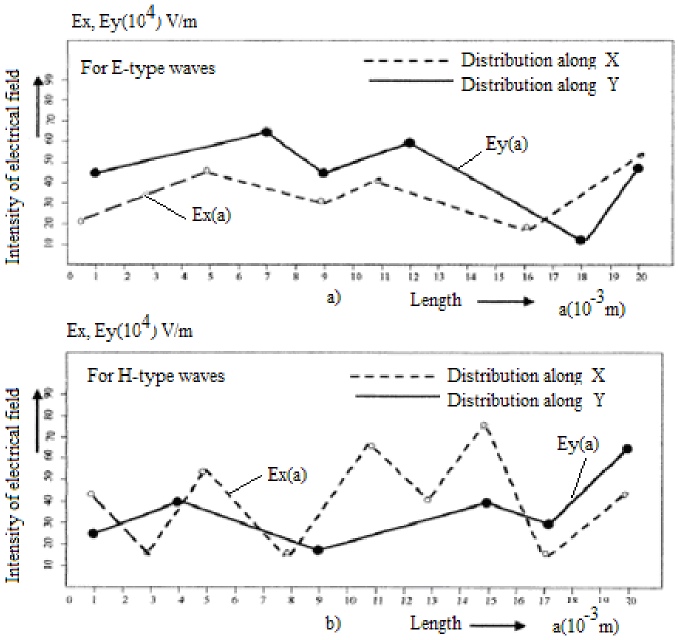

Fig.8 The relationships between the electric field strength and the length of the cross-section of RW with air filling for the E-type (a) and the H-type (b) of the waves according to the results of experimental research.

Based on the experimental data, the relationship between electric field intensity and the length of the cross-section of RW with air filling for the E-type (fig.8, a) and the H-type (fig.8, b) waves. These relationships allow us to determine the electric field distribution inside the device.

It should be noted that to get the true value of E the measurements must be repeated for n> 30 times. Therefore, considering these conditions for each elementary area, the measurements were repeated for n = 45 times. After receiving the experimental data in the form of statistical series and analysis, errors were ruled out for serious mistakes and then the measurement was repeated for such cases. The total measurement error is ± 4,35%. A discrepancy between theory and experiment is about 5%. Comparing the results of the calculation of the electric field RW with air filling in the formula (9) with the experimental data, we can see that the differences in the numerical values of E are practically acceptable. This fact proves not only the correctness of the obtained results by the formula (9), and reaffirms the importance of the proposed formula, which provides an extremely simple solution to a complex problem. On the basis of the obtained results the following conclusions can be made.

VI. CONCLUSIONS

1. It is shown that in strong fields, the environment inside of RW with air filling behaves non-linearly, ie. relative dielectric conductivity of environment ε is a strength function of the electric field E.
2. Taking the nonlinearity of the medium into account, it was constructed new mathematical model of the electric field RW with air filling operating at frequencies 4,9 ÷ 7,05 GHz.
3. The resulting non-linear differential equation is solved using the finite difference method and it was determined the numerical values of the electric field of RW with air filling for the excitation E-type and H-type waves.
4. Conducted an experimental study of the electric field inside of RW with air filling. This confirmed the

theoretical results obtained in this work. This proves not only faithfulness to the results, but also the importance of the proposed formula, which provides an extremely simple solution to a complex problem.

5. Theoretical and experimental results obtained in this study can be used in a variety of television towers, which gives an opportunity to significantly increase productivity while controlling and measuring operations.

REFERENCES

[1]. I.J.Islamov. Transaction of Azerbaijan Academy of Sciences, Series of Physical-mathematical and Technical sciences, Physics and Astronomy, XXIV №2 (2004) 48-57.

[2]. I.J.Islamov. Transaction of Azerbaijan Academy of Sciences, Series of Physical-mathematical and Technical sciences, Physics and Astronomy, XXIII №2 (2003) 205-214.

[3]. E.G.Ismibayli, I.J.Islamov, Y.G.Gaziyev. Calculation Of The Electromagnetic Field Of The Microwave Of Devices With Use Of Method FDTD And Integral Kirchhoff. International Journal of Engineering Innovation and Research (IJEIR), Volume 5, Issue 1, (2016) 103-106.

[4]. E.G.Ismibayli, I.J.Islamov, Y.G.Gaziyev. Modeling Of Electromagnetic Fields Of Microwave Devices On The Basis Of Matlab Program. International Journal of Innovative Science, Engineering and Technology (IJISET), Volume 3, Issue 2, (2016) 61-63.

[5]. E.G.Ismibayli, I.J.Islamov, Y.G.Gaziyev. An Optimal Control Of An Electromagnetic Field In High-Powered Microwave Devices. International Journal of Trend in Research and Development (IJTRD), Volume 3(1), (2016) 246-249.

[6]. E.G.Ismibayli, I.J.Islamov, Y.G.Gaziyev. Modeling of Anisotropic Rectangular Waveguide Partially Embedded in an Anisotropic Substrate. Journal of Multidisciplinary Engineering Science and Technology (JMEST). Volume 2, Issue 2, (2015) 153-157.

[7]. Islam J. Islamov. Application of finite elements method by calculating electric field of hollow rectangular waveguide. IASTED-2005, Canada, Calgary, (2005) 26-32.

[8]. Islam J. Islamov. Numerical method for analysis of electromagnetic field of microwave waveguide. International Conference on Antenna Theory and Techniques. September 9-12, Sevastopol, Ukraine, (2003) 45-50.

[9]. E.G. Ismibeyli, I.D. Islamov. The Analysis of Magnetic Devices In Frequency Directors of Teledynamometring Systems. The Third International Scientific Practical Conference "Khazarneftgasyatag-98", November, Baku, (1998) 10-13.

[10]. De Moerloose Jan, Dawson Trevor W., Stuchly Maria A. Application of the finite difference time domain algorithm to quasi-static field analysis. Radio Sci.-32, №2 (1997) 329-341.

[11]. M.Koshiba, M.Okada, M.Suzuki. Numerical analysis of two-dimensional piezoelectric waveguides for surface acoustic waves by finite-element method. “Electron. Lett.”, №17 (1981) 609-611.

[12]. Y.E.Elmoazzen, Shafai Lotfollah. Numerical solution of coupling between two collinear parallel-plate waveguides. IEEE Trans. Microwave Theory and Techn., 23(11), (1975) 871-876.

[13]. T.P.Barton. Electromagnetic field calculations for irregularly shaped, layered cylindrical particles with focused illumination. Appl. Opt., 36, (1997) 1312-1319.

[14]. V.Iomota, P.Alotto. Magnetic field computation in media with hysteresis. Rev. roum. sci. techn. Ser. Electrotechn. et energ. 41(3), (1996) 291-296.

[15]. K. Dikshitulu Kalluri. Elektromaqnetic Waves. Materials and computation with Matlab. CRS Press London-New York, (2012) 835.

[16]. N.O.Matthew Sadiku. Numerical Techniques in Electromagnetic with Matlab. CRS Press London-New York, (2012) 707.

[17]. Munteanu Irina. A method for numerically solving Maxwell's equations in three dimension. Politehn. Univ. Bucharest. 56(1-4), (1994) 221- 238.

[18]. Miller Edmund K., Burke Gerald J. Low frequency computational electromagnetics for antenna analysis. Proc. IEEE. 80(1), (1992) 24-43.

[19]. Chen Bao Xue, Hamanaka Hiromi, Iwamura Kokya. J. Opt. Soc. Amer. 9(8), (1992) 1301-1305.

[20]. H.Cory, A.Novick-Cohen, D.Levy. Variational expression for propagation along a closed rectangular chiro waveguide. Antennas and Propag., 143(2), (1996) 174-178.

[21]. B.N.Das., S.B.Chakrabarty. Analysis of a pair of dielectric coated above a dielectric substrate. IEE Proc. Microwaves, Antennas and Propag.143(1), (1996) 67-72.

[22]. A.Larer, I.Donets, S.Bryzgalo. The semi inversion method for cylindrical microwave structures. Jour. of electromagnetic Waves and Application, 10(6), (1996) 765-790.